Journal of Engineering Mathematics 21: 101–114 (1987)

A note on a Galerkin technique for integral equations in potential flows

P.D. SCLAVOUNOS
Department of Ocean Engineering, Massachusetts Institute of Technology, Cambridge, MA 02139, USA

Received 4 November 1986; accepted 25 November 1986

Abstract

The properties are studied of a Galerkin numerical solution of integral equations for an assumed singularity distribution or a velocity potential arising in potential flows around rigid bodies in incompressible aerodynamics, acoustics and surface waves. The body boundary is approximated by a collection of panels and the integral equation is averaged over each panel instead of being enforced at a 'collocation' point. For the resulting Galerkin synthesis the matrix equation obtained for the source distribution is the exact transpose of the corresponding equation obtained for the velocity potential on the body boundary, a property known to hold for the continuous operators. Moreover, the integrated hydrodynamic forces experienced by the body are shown to be identically predicted by the source-distribution method or by directly solving for the velocity potential.

1. Introduction

The foundation of surface integral equations in potential flows goes back to the famous identity of Green. Different formulations in terms of surface singularity distributions are derived by Lamb [1], but it was only until about twenty years ago that the advent of electronic computers permitted their use in practice. The pioneering work of Hess and Smith [2] is the first successful numerical implementation of surface-singularity integral equations in a three-dimensional problem. Numerous applications have since appeared in aerodynamics, acoustics, electromagnetics and surface-wave flows.

Given our task to determine a potential function on the body boundary, two are the most widely used forms of boundary integral equations. The 'source-distribution' method represents the potential as a distribution of source singularities on the body boundary. Their strength is determined by the solution of an integral equation on its surface by enforcing the relevant boundary condition. This is hereafter assumed to be of the Neumann type. Alternatively, an integral equation for the potential function itself can be obtained over the body boundary. This is often called the 'Green' method. A rational derivation of both formulations is given in [1].

The simplest numerical approximation of either method requires the representation of the body boundary by a collection of plane quadrilaterals, or panels, with the source distribution or potential function itself assumed constant over their surface. The integral equations are satisfied at 'collocation' points located on each panel, often selected to be at their centroid. The continuous problem is reduced to a matrix equation with as many unknowns as the number of panels used to approximate the body boundary, if symmetries are not accounted for. The typical matrix element represents the hydrodynamic influence between a pair of panels. This

synthesis in connection with the source-distribution method, has been implemented with remarkable success by Hess and Smith [2] for incompressible non-lifting flows past three-dimensional bodies. The alternative Green method has been later advocated in aerodynamics by Morino and Kuo [3] with similar success. Numerous applications of both methods are also known in acoustics and surface-wave body interactions.

In the continuous problem, the two alternative integral equations have transpose kernels and possess identical solutions for the potential function. A proof is given in Section 2. Neither property is preserved in the discrete problem if the collocation method is implemented. Computations suggest that for a sufficiently fine discretization, the solutions of the two equations are 'close' but are not identical. The Galerkin method studied in the present paper brings closer the discrete solutions of the source-distribution and Green methods. The integral equation is averaged over the surface of each panel instead of being satisfied at a single collocation point. This procedure restores one of the properties of the continuous problem, in that it leads to matrix equations for the source-distribution and the Green methods which are the exact transpose of each other. The respective solutions for the potential function are not identical, but the integrated hydrodynamic forces on the body boundary are. Numerical experiments indicate that the difference between the potential functions predicted by the two methods when the Galerkin technique is used is smaller than the corresponding difference in the collocation method. The proof of these properties is derived in Section 3.

The computational effort required in the implementation of the Galerkin technique and aspects pertaining to its use in practice are discussed in Section 4.

2. The continuous problem

An inertial Cartesian coordinate system (x, y, z) and a rigid body fixed relative to it are defined in Fig. 1.

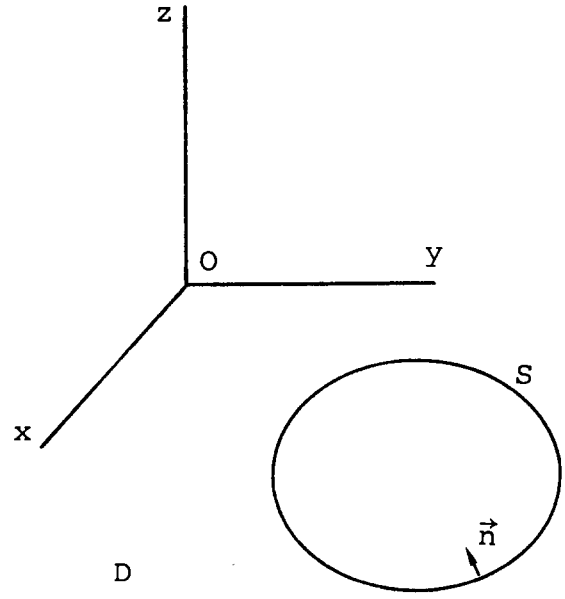

Fig. 1

We are interested in determining the potential function ϕ on the surface S of the body, subject to

$$\phi_{xx} + \phi_{yy} + \phi_{zz} + k^2\phi = 0 \tag{2.1}$$

in the domain D, where k is a real constant and

$$\frac{\partial\phi}{\partial n} = V \tag{2.2}$$

on the body boundary, where the normal vector $\mathbf{n}$ is of unit length and points out of the domain D.

At large radial distances form the origin O a condition needs to be satisfied by the potential ϕ, specific to the problem being analysed. In the incompressible limit $k = 0$, if the potential represents the disturbance due to an incident flow, it is subject to the condition

$$\nabla\phi \to 0 \tag{2.3}$$

at infinity. For compressible potential flows, the Helmholtz equation (2.1) models the linearized time-harmonic problem for which a Sommerfeld radiation condition of outgoing waves is necessary for the disturbance potential, $\phi = \mathrm{Re}(\varphi\, \mathrm{e}^{\mathrm{i}\omega t})$, where ω is the frequency of oscillation,

$$r^{1/2}\left(\frac{\partial\varphi}{\partial r} - \mathrm{i}k\varphi\right) \to 0 \tag{2.4}$$

for large $r = (x^2 + y^2 + z^2)^{1/2}$. If a free-surface flow is being analysed, with the calm free surface assumed to be the $z = 0$ plane, $k = 0$ in (2.1) and the disturbance wave potential satisfies

$$\varphi_z - k\varphi = 0 \tag{2.5}$$

on $z = 0$. The relevant conditions at infinity are the Sommerfeld radiation condition with r replaced by $R = (x^2 + y^2)^{1/2}$, and

$$\nabla\varphi \to 0 \tag{2.6}$$

as z tends to $-\infty$. If additional rigid boundaries are present, the normal velocity needs to be specified on their surface.

The solution of the boundary-value problems (2.1)–(2.6) by surface integral equations has gained a lot of popularity in recent years. They lead to the discretization of a two-dimensional surface, treat domains of infinite extent and are algorithmically easy to implement. Their derivation originates from Green's theorem. Two formulations have received considerable attention because they lead to the numerical solution of Fredholm integral equations of the second kind which produce well-conditioned linear systems.

Historically, the 'source-distribution' method appears to have been analysed first, perhaps because of its relation to the theory of gravitation. The potential is represented by a distribution of sources and sinks on the body boundary in the form

$$\varphi(\mathbf{x}) = \int_S \mathrm{d}\xi\sigma(\xi)G(\mathbf{x};\,\xi). \tag{2.7}$$

The 'Green function' $G(\mathbf{x};\ \boldsymbol{\xi})$ represents the potential at the field point $\mathbf{x} = (x,\ y,\ z)$ due to a unit source located at the point $\boldsymbol{\xi} = (\xi,\ \eta,\ \zeta)$. It satisfies equations (2.1) and (2.2)–(2.6) with the exception of the body boundary condition (2.2).

For incompressible three-dimensional flows, G is often referred to as the Rankine singularity and is defined by

$$G(\mathbf{x};\ \boldsymbol{\xi}) = -\frac{1}{4\pi r}, \tag{2.8}$$

where r is the radial distance between the source and field points. For time-harmonic acoustic flows,

$$G(\mathbf{x};\ \boldsymbol{\xi}) = -\frac{1}{4\pi r} e^{-ikr}, \tag{2.9}$$

and for time-harmonic free-surface flows in infinite water depth

$$G(\mathbf{x};\ \boldsymbol{\xi}) = -\frac{1}{4\pi}\left(\frac{1}{r} + \frac{1}{r'}\right) + \tfrac{1}{2}i\, e^{k(z+\zeta)} J_0(kR) - \frac{1}{4\pi}\int_0^\infty \frac{s+1}{s-1} e^{s(z+\zeta)} J_0(sR)\, ds, \tag{2.10}$$

where r' is the radial distance from the image of the source point with respect to the $z = 0$ plane to the field point $\mathbf{x}$ and J_0 is the Bessel function of the first kind of order zero. The Green function (2.10) is derived in Wehausen and Laitone [4], together with its expression in water of uniform finite depth. In time-harmonic flows the real part of the product of all complex quantities with the time factor $e^{i\omega t}$ is understood. A set of efficient algorithms for the evaluation of the Green function (2.10) has been recently developed and coded by Newman [5].

Enforcing the boundary condition (2.2) on the body boundary, assumed to possess a continuous slope, leads to an integral equation for the source strength $\sigma(\mathbf{x})$ on its surface:

$$-\tfrac{1}{2}\sigma(\mathbf{x}) + \int_S d\boldsymbol{\xi}\sigma(\boldsymbol{\xi})\frac{\partial G(\mathbf{x};\ \boldsymbol{\xi})}{\partial n_{\mathbf{x}}} = V(\mathbf{x}). \tag{2.11}$$

The pair of equations (2.7) and (2.11) define the 'source-distribution method'.

The alternative 'Green method' solves directly for the potential $\varphi(\mathbf{x})$ on the body boundary. The corresponding integral equation is Green's identity itself:

$$-\tfrac{1}{2}\varphi(\mathbf{x}) + \int_S d\boldsymbol{\xi}\varphi(\boldsymbol{\xi})\frac{\partial G(\boldsymbol{\xi};\ \mathbf{x})}{\partial n_{\boldsymbol{\xi}}} = \int_S d\boldsymbol{\xi} V(\boldsymbol{\xi}) G(\boldsymbol{\xi};\ \mathbf{x}). \tag{2.12}$$

Values of $\varphi(\mathbf{x})$ with $\mathbf{x}$ in the fluid domain can be obtained from equation (2.12) by replacing the leading coefficient $-1/2$ by -1, following the solution of (2.12) which determines its values on the body boundary.

The solutions of the continuous equations (2.7), (2.11) and (2.12) for the velocity potential $\varphi(\mathbf{x})$ on the body boundary are identical. The proof is based on the existence and uniqueness of the solution to the boundary-value problems (2.1)–(2.6), alternative formulations of which are offered by the two transpose integral formulations. Care is needed to validate this statement in the wave problems at a discrete set of 'resonant frequencies' which lead to the vanishing of the Fredholm determinant of the respective integral equations. A comprehensive study of this subject is carried out in the book by Colton and Kress [6].

An operator proof is given here of the identity of the two solutions based on the application of Green's theorem. The intention is to motivate the discussion of the discrete problem where

the continuous integral operators are approximated by matrices. Rewrite equations (2.7) and (2.11) in the form

$$\varphi = S\sigma, \tag{2.13}$$

$$D_s\sigma = V, \tag{2.14}$$

and equation (2.12) in the form

$$D_G\varphi = SV, \tag{2.15}$$

where S, $D_{S,G}$ is the operator notation of the respective integral representations, $V = V(\mathbf{x})$ is the normal velocity specified on the body boundary and $\varphi = \varphi(\mathbf{x})$ the desired potential. By definition, the operators D_S and D_G are the transpose of each other, thus

$$D_S = D_G^T, \tag{2.16}$$

and by virtue of the symmetry of the Green function $G(\mathbf{x}; \boldsymbol{\xi})$ with respect to its arguments,

$$S = S^T. \tag{2.17}$$

A necessary condition for the solutions of (2.13)–(2.14) and (2.15) to be identical is obtained by replacing V in the right-hand side of (2.15) by its definition in (2.14) and by operating on both sides of (2.13) by D_G. In operator form the result is

$$D_G S = SD_S. \tag{2.18}$$

Transposing both sides of (2.18) produces the same equation, by virtue of (2.16) and (2.17).

To prove (2.18), we operate separately with the left- and right-hand side operators on an arbitrary, sufficiently smooth, function $f = f(\mathbf{x})$ defined on the body boundary. By definition,

$$(D_G S)f = \int_{S+S_\epsilon} \mathrm{d}\xi \frac{\partial G(\xi; \mathbf{x})}{\partial n_\xi} \int_{S+S'_\epsilon} \mathrm{d}\xi' f(\xi') G(\xi; \xi'), \tag{2.20}$$

and

$$(SD_S)f = \int_{S+S_\epsilon} \mathrm{d}\xi G(\mathbf{x}; \xi) \int_{S+S'_\epsilon} \mathrm{d}\xi' f(\xi') \frac{\partial G(\xi; \xi')}{\partial n_\xi}. \tag{2.21}$$

The leading terms in (2.11) and (2.12) have been replaced by the integrals over the surfaces S_ϵ and S'_ϵ which are half spheres of small radius ϵ and are illustrated in Fig. 2.

In the limit $\epsilon \to 0$, the contributions from these surfaces tend to the leading terms of (2.11) and (2.12) for the integrands which involve a normal derivative of the Green function, or vanish when the integrands that involve the Green function itself. Define the potentials

$$\varphi_1(\xi) = G(\xi; \mathbf{x}), \tag{2.22}$$

$$\varphi_2(\xi) = \int_{S+S'_\epsilon} \mathrm{d}\xi' f(\xi') G(\xi; \xi'). \tag{2.23}$$

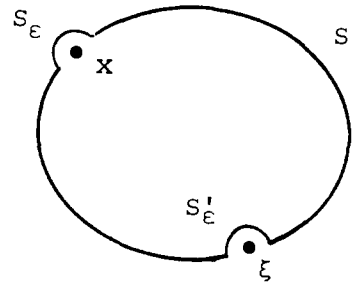

Fig. 2

Both satisfy the field equation. Substituting (2.22)–(2.23) in (2.20) and (2.21) we obtain respectively,

$$(D_G S)f = \int_{S+S_\epsilon} d\xi \frac{\partial \varphi_1(\xi)}{\partial n_\xi} \varphi_2(\xi), \tag{2.24}$$

$$(SD_S)f = \int_{S+S_\epsilon} d\xi \varphi_1(\xi) \frac{\partial \varphi_2(\xi)}{\partial n_\xi}. \tag{2.25}$$

The right-hand sides of (2.24), (2.25) are equal by virtue of Green's identity. This concludes the proof of (2.18) which is a necessary condition for the identity of the solution of the source-distribution and the Green methods. To establish that it is also sufficient, the operators $D_{S,G}$ must not be singular. The solution of (2.13)–(2.14) can be written in the form

$$\varphi_S = (SD_S^{-1})V, \tag{2.26}$$

and that of (2.15) in the form

$$\varphi_G = (D_G^{-1}S)V. \tag{2.27}$$

The equality

$$SD_S^{-1} = D_G^{-1}S \tag{2.28}$$

follows from (2.18) by pre-operating on both sides D_G and post-operating by D_S.

3. The discrete problem

The discretization errors in the numerical solution of the integral equations of Section 2 originate from the approximation of the body surface by panels, the approximate representation of the source strength or velocity potential on the panels, the way in which the integral equation is satisfied, quadrature errors in the evaluation of integrals of the Green function and its derivatives over the panels.

Roundoff errors are also present in the set-up and solution of the resulting linear system on a digital computer. The effect of the discretization and roundoff error on the solution is proportional to their magnitude and the conditioning of the Fredholm integral equation of the second kind being solved. This is generally good, as is illustrated by the small condition number of the matrices approximating the integral equations and its weak dependence on the number of panels that approximate the body surface.

The selection of plane quadrilaterals with the unknown function assumed to be piecewise constant over their surface is quite popular in production panel codes intended for the analysis of bodies of general shape. The integral equation is satisfied at a set of 'collocation' points often located at the panel centroids. Hess and Smith [2] pioneered the way in aerodynamics by implementing this framework in connection with the source-distribution method and Morino and Kuo [3] in connection with the Green method. Numerous applications have appeared since in acoustics and wave-body interactions. The additional complication in these problems is the presence of the irregular frequencies, and in the latter the complexity in the computation of the wave Green function defined by (2.10).

The use of the source-distribution versus the Green method depends on a number of factors specific to the problem of interest. Some of them are discussed in Section 4. The numerical solutions obtained from the two methods by applying point collocation are not identical. They are affected to a different extent by the discretization errors present in both methods. Their difference can be reduced if the selection of a single collocation point is replaced by the Galerkin technique which instead averages the integral equation over the surface of each panel. The merits of the latter method, not shared by the collocation method, are:

1. the symmetry of the operator S and the transpose relation between the operators D_S and D_G are present in their discrete approximations by matrices;
2. the integrated hydrodynamic forces on the body obtained by the two methods are identical.

Denote by s_i the surface of the i-th quadrilateral and by a_i its area. Discretizing the pair of equations (2.13)–(2.14) on the assumption that the source distribution is constant over the surface of each panel, followed by an averaging with respect to the x-coordinate over their surface, we obtain for the source-distribution method

$$\varphi_i = \frac{1}{a_i} \sum_{j=1}^{N} S_{ij}\sigma_j, \tag{3.1}$$

$$-\tfrac{1}{2}\sigma_i a_i + \sum_{j=1}^{N} D_{ij}^{(S)}\sigma_j = a_i V_i, \quad i = 1, \ldots, N, \tag{3.2}$$

where the matrices S_{ij} and $D_{ij}^{(S)}$ are defined by

$$S_{ij} = \int_{s_i} \mathrm{d}\mathbf{x} \int_{s_j} \mathrm{d}\boldsymbol{\xi} G(\mathbf{x}; \boldsymbol{\xi}), \tag{3.3}$$

$$D_{ij}^{(S)} = \int_{s_i} \mathrm{d}\mathbf{x} \int_{s_j} \mathrm{d}\boldsymbol{\xi} \frac{\partial G(\mathbf{x}; \boldsymbol{\xi})}{\partial n_{\mathbf{x}}}. \tag{3.4}$$

The same procedure applied to the Green equation (2.15) leads to

$$-\tfrac{1}{2}\varphi_i a_i + \sum_{j=1}^{N} D_{ij}^{(G)}\varphi_j = \sum_{j=1}^{N} S_{ij} V_j, \quad i = 1, \ldots, N, \tag{3.5}$$

where

$$D_{ij}^{(G)} = \int_{s_i} \mathrm{d}\mathbf{x} \int_{s_j} \mathrm{d}\boldsymbol{\xi} \frac{\partial G(\boldsymbol{\xi}; \mathbf{x})}{\partial n_{\boldsymbol{\xi}}}. \tag{3.6}$$

Matrices S_{ij} and $D_{ij}^{(S),(G)}$ are the discrete analogs of the integral operators defined in Section 2. It is easy to verify that

$$S_{ij} = S_{ji}, \tag{3.7}$$

resulting from the symmetry of the Green function with respect to its arguments.

Matrices $D^{(S)}$ and $D^{(G)}$ are the transpose of each other,

$$D_{ij}^{(S)} = D_{ji}^{(G)}. \tag{3.8}$$

The proof of (3.8) follows after the dummy variables in the double integral (3.6) and the indices i and j are interchanged. Relations (3.7) and (3.8) are the discrete analogs of the corresponding relations (2.17) and (2.16) in the continuous problem.

We turn our attention to the solutions for the velocity potentials obtained from the two discrete formulations (3.1)–(3.4) and (3.5)–(3.6). Define

$$A = \text{diag}(a_i), \tag{3.9}$$

$$D = -\tfrac{1}{2}A + D^{(G)}, \tag{3.10}$$

and express the solution potential from the source-distribution method in the form

$$\boldsymbol{\varphi}^{(S)} = A^{-1}S(D^T)^{-1}A\mathbf{v}, \tag{3.10}$$

and from the Green method

$$\boldsymbol{\varphi}^{(G)} = D^{-1}S\mathbf{v}. \tag{3.11}$$

For an arbitrary normal-velocity vector $\mathbf{v}$, the two solutions would be identical if the matrices multiplying $\mathbf{v}$ in (3.10) and (3.11) are equal, or equivalently if the matrix

$$W = AD^{-1}S \tag{3.12}$$

is symmetric. The proof that W is symmetric did not prove possible. Numerical experiments for a model problem in two dimensions with the Laplace equation satisfied in the fluid domain indicate that W is 'almost symmetric', meaning that elements with symmetric locations relative to the principle diagonal agree to 2–3 digits. A similar agreement was verified for the velocity potential obtained from the two methods. The symmetry of W would be equivalent to the condition (2.28) in the continuous problem. This can be seen if the matrix A is set equal to the unit matrix, and by equating the remaining matrix product by its transpose.

In interactions of linear surface waves with bodies, the knowledge of the integrated hydrodynamic pressure over the body wetted surface is often more interesting than the knowledge of the velocity potential itself. The hydrodynamic force can be obtained by integrating over the body surface the product of the panel area by the solution velocity potential and the vector $\mathbf{u}$ which represents the 'direction' of the force we are interested to evaluate. This operation is equivalent to the pre-multiplication of the vector velocity potential by the vector $(A\mathbf{u})^T$. The resulting hydrodynamic force obtained from the source distribution method is given by

$$H_{\mathbf{uv}}^{(S)} = \mathbf{u}^T W^T \mathbf{v}. \tag{3.13}$$

The same force predicted by the Green method takes the form

$$H_{\mathbf{uv}}^{(G)} = \mathbf{u}^T W \mathbf{v}. \tag{3.14}$$

Since the quantities H are scalars, we obtain by transposing (3.14) and interchanging the vectors **u** and **v**:

$$H_{\mathbf{uv}}^{(S)} = H_{\mathbf{uv}}^{(G)}. \tag{3.15}$$

It follows that:

1. If $\mathbf{u} = \mathbf{v}$ the hydrodynamic force predicted by the source-distribution method is identical to the same force predicted by the Green method;
2. More generally, the hydrodynamic force in the **v**-direction due to forcing in the **u**-direction predicted by one method is identical to the force in the **u**-direction due to forcing in the **v**-direction predicted by the other.

The properties derived in the present section are not shared by the collocation method in which the lack of the surface integral with respect to the **x**-coordinates prevents the symmetry of matrix S and the transpose relation between the matrices $D^{(S),(G)}$.

4. Numerical results

This section presents numerical results for the source strength, velocity potential distribution and added mass of an ellipse translating in an infinite fluid, documenting the performance of the collocation and Galerkin methods. In Fig. 3, N equal increments of the angle α from 0 to 2π define an equal number of vertices on the ellipse surface spaced in cosine-like manner. Straight segments are used to connect adjacent vertices. Denote by σ the source strength distribution and φ the corresponding velocity potential (related by equation (2.7)) due to the ellipse translation in the direction of its major axis with a unit velocity. Let $\mathbf{n} = (n_1, n_2)$ be the inwards-pointing unit vector.

The exact continuous values for the velocity potential are given by

$$\frac{\varphi(\alpha)}{UB/2} = -\epsilon \cos \alpha, \tag{4.1}$$

and for the added-mass coefficient A_{11},

$$\frac{A_{11}}{\rho B^2/4} = \pi\epsilon^2, \tag{4.2}$$

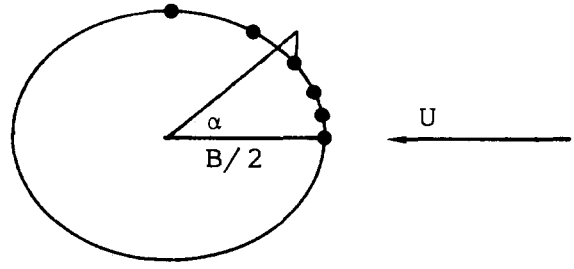

Fig. 3

Table 1. Source-strength, velocity potential distributions and added mass of an ellipse of eccentricity 0.5 discretized by 32 straight segments, using the collocation method.

i	x-midpoint	y-midpoint	SIGMA	PHI	EXACT PHI	ERROR (%)
1	0.990	0.049	1.573	−0.521	−0.495	5.18
2	0.952	0.144	1.353	−0.499	−0.476	4.89
3	0.878	0.235	1.064	−0.459	−0.439	4.50
4	0.769	0.316	0.801	−0.400	−0.385	4.12
5	0.631	0.385	0.580	−0.328	−0.316	3.82
6	0.469	0.439	0.393	−0.243	−0.235	3.61
7	0.289	0.476	0.227	−0.149	−0.144	3.47
8	0.098	0.495	0.075	−0.050	−0.049	3.40
9	−0.098	0.495	−0.075	0.050	0.049	3.40
10	−0.289	0.476	−0.227	0.149	0.144	3.47
11	−0.469	0.439	−0.393	0.243	0.235	3.61
12	−0.631	0.385	−0.580	0.328	0.316	3.82
13	−0.769	0.316	−0.801	0.400	0.385	4.12
14	−0.878	0.235	−1.064	0.459	0.439	4.50
15	−0.952	0.144	−1.353	0.499	0.476	4.89
16	−0.990	0.049	−1.573	0.521	0.495	5.18
17	−0.990	−0.049	−1.573	0.521	0.495	5.18
18	−0.952	−0.144	−1.353	0.499	0.476	4.89
19	−0.878	−0.235	−1.064	0.459	0.439	4.50
20	−0.769	−0.316	−0.801	0.400	0.385	4.12
21	−0.631	−0.385	−0.580	0.328	0.316	3.82
22	−0.469	−0.439	−0.393	0.243	0.235	3.61
23	−0.289	−0.476	−0.227	0.149	0.144	3.47
24	−0.098	−0.495	−0.075	0.050	0.049	3.40
25	0.098	−0.495	0.075	−0.050	−0.049	3.40
26	0.289	−0.476	0.227	−0.149	−0.144	3.47
27	0.469	−0.439	0.393	−0.243	−0.235	3.61
28	0.631	−0.385	0.580	−0.328	−0.316	3.82
29	0.769	−0.316	0.801	−0.400	−0.385	4.12
30	0.878	−0.235	1.064	−0.459	−0.439	4.50
31	0.952	−0.144	1.353	−0.499	−0.476	4.89
32	0.990	−0.049	1.573	−0.521	−0.495	5.18

added mass = 0.8159
exact added mass = 0.7854
relative error = 3.89%

where ϵ is the ratio of the minor to the major ellipse axes. To test the performance of the Galerkin technique, the discrete set of equations (3.2) has been solved for the source strength and the velocity potential has been evaluated from equations (3.1). Table 1 presents predictions from the collocation method of the source strength (SIGMA), velocity potential (PHI) and errors relative to the exact velocity potential for an ellipse of eccentricity $\epsilon = 0.5$ discretized by 32 segments. The exact values of the velocity potential are evaluated from (4.1) at half-increments of the angle α. The relative error for the velocity potential ranges from 3–5%. The corresponding predictions of the Galerkin method are presented in Table 2 for the same number of segments. The errors in the velocity potential predictions now range from 0.18–0.75%, and for the added mass it is equal to −0.14%.

Added-mass predictions for ellipses of varying eccentricity ratios and number of segments are presented in Table 3 for the collocation, and Table 4 for the Galerkin method. It is here reminded that the Galerkin added masses obtained by utilizing the source-distribution and the Green methods are identical.

The numerical results presented in Tables 1–4 have been obtained by Barnel [7]. In both methods, all integrals of the Green function log r and its normal derivative over the segments

Table 2. Source-strength, velocity potential distributions and added mass of an ellipse of eccentricity 0.5 discretized by 32 straight segments, using the Galerkin method.

i	*x*-midpoint	*y*-midpoint	SIGMA	PHI	EXACT PHI	ERROR (%)
1	0.990	0.049	1.491	−0.499	−0.495	0.75
2	0.952	0.144	1.289	−0.479	−0.476	0.60
3	0.878	0.235	1.024	−0.441	−0.439	0.44
4	0.769	0.316	0.779	−0.386	−0.385	0.33
5	0.631	0.385	0.568	−0.316	−0.316	0.26
6	0.469	0.439	0.386	−0.235	−0.235	0.21
7	0.289	0.476	0.224	−0.145	−0.144	0.19
8	0.098	0.495	0.074	−0.049	−0.049	0.18
9	−0.098	0.495	−0.074	0.049	0.049	0.18
10	−0.289	0.476	−0.224	0.145	0.144	0.19
11	−0.469	0.439	−0.386	0.235	0.235	0.21
12	−0.631	0.385	−0.568	0.316	0.316	0.26
13	−0.769	0.316	−0.779	0.386	0.385	0.33
14	−0.878	0.235	−1.024	0.441	0.439	0.44
15	−0.952	0.144	−1.289	0.479	0.476	0.60
16	−0.990	0.049	−1.491	0.499	0.495	0.75
17	−0.990	−0.049	−1.491	0.499	0.495	0.75
18	−0.952	−0.144	−1.289	0.479	0.476	0.60
19	−0.878	−0.235	−1.024	0.441	0.439	0.44
20	−0.769	−0.316	−0.779	0.386	0.385	0.33
21	−0.631	−0.385	−0.568	0.316	0.316	0.26
22	−0.469	−0.439	−0.386	0.235	0.235	0.21
23	−0.289	−0.476	−0.224	0.145	0.144	0.19
24	−0.098	−0.495	−0.074	0.049	0.049	0.18
25	0.098	−0.495	0.074	−0.049	−0.049	0.18
26	0.289	−0.476	0.224	−0.145	−0.144	0.19
27	0.469	−0.439	0.386	−0.235	−0.235	0.21
28	0.631	−0.385	0.568	−0.316	−0.316	0.26
29	0.769	−0.316	0.779	−0.386	−0.385	0.33
30	0.787	−0.235	1.024	−0.441	−0.439	0.44
31	0.952	−0.144	1.289	−0.479	−0.476	0.60
32	0.990	−0.049	1.491	−0.499	−0.495	0.75

added mass = 0.7843
exact added mass = 0.7854
relative errror = −0.14%

have been evaluated in closed form. Consequently, only discretization errors due to the approximation of the ellipse by straight segments and the representation of the unknown source strength by a piecewise-constant variation are present. Roundoff errors in the solution of the linear systems are negligible for the number of segments used in these examples. It may be concluded that the use of the Galerkin method leads to a substantial decrease of discretization errors, here typically by a factor of ten. More recent results for two-dimensional hydrofoil flows indicate a similar improvement in accuracy relative to the collocation method.

In three dimensions the Galerkin method has been used by Breit, Newman and Sclavounos [8] in the evaluation of the complex-impedance hydrodynamic coefficients of a surface-piercing spheroid and a truncated vertical cylinder approximated by plane quadrilaterals. An improvement in accuracy relative to the collocation method has been observed, but a more modest one in comparison to that typically observed in two dimensions. In three dimensions the double Galerkin integrals of the Rankine source (2.8) and both single and double integrals of the wave Green function (2.10) and its derivatives over plane quadrilaterals do not possess closed-form expressions, and a four-node surface Gauss quadrature was utilized. In all cases tested the

Table 3. Added mass of ellipses for eccentricities ranging from 0.1 to 1.0 discretized with 16, 32 and 48 segments using the collocation method.

n	ϵ	ADDED MASS	EXACT ADDED MASS	ERROR (%)
16	0.10	0.033	0.031	4.81
32	0.10	0.033	0.031	4.01
48	0.10	0.032	0.031	2.86
16	0.20	0.134	0.126	6.69
32	0.20	0.131	0.126	4.04
48	0.20	0.129	0.126	2.77
16	0.30	0.302	0.283	6.92
32	0.30	0.294	0.283	3.96
48	0.30	0.290	0.283	2.73
16	0.40	0.537	0.503	6.88
32	0.40	0.522	0.503	3.91
48	0.40	0.516	0.503	2.71
16	0.50	0.839	0.785	6.81
32	0.50	0.816	0.785	3.89
48	0.50	0.807	0.785	2.69
16	0.60	1.175	1.131	3.87
48	0.60	1.161	1.131	2.69
16	0.70	1.643	1.539	6.73
32	0.70	1.599	1.539	3.87
48	0.70	1.581	1.539	2.68
16	0.80	2.146	2.011	6.72
32	0.80	2.088	2.011	3.86
48	0.80	2.065	2.011	2.68
16	0.90	2.715	2.545	6.71
32	0.90	2.643	2.545	3.86
48	0.90	2.613	2.545	2.68
16	1.00	3.352	3.142	6.71
32	1.00	3.263	3.142	3.86
48	1.00	3.226	3.142	2.68

quadrature errors were found to be small relative to the discretization errors associated with the approximation of the geometry and the unknown velocity potential or source distributions.

5. Application of the Galerkin method

The computational effort required for the evaluation of the Galerkin matrices is not substantially larger than the corresponding effort in the collocation method. The integral with respect to the **x**-coordinate can be evaluated by quadrature. When the panels i and j are located at a distance from each other comparable to their typical dimension, the variation of the integral over the j-th panel, being function of the **x**-coordinate, is in principle rapid as the point **x** spans the area of the i-th panel. It is due to the singular behaviour of all Green functions defined in Section 2. Consequently, more than one quadrature points are likely to be necessary over the surface of the i-th panel in the evaluation of the double integrals (3.3) and (3.4), leading to an increase in the computational effort relative to the collocation method.

When the panels i and j are at large a distance from each other relative to their typical dimension, the variation of the Green function $G(\mathbf{x}; \boldsymbol{\xi})$ and its derivatives over their surfaces s_i and s_j is gradual. A single-node quadrature is adequate in this case for the evaluation of the double integrals, with the node located on the panel centroid. Thus, a single evaluation of the Green function and its derivatives is necessary for each element of the matrices S and D, as in the collocation method. If the effort in the evaluation of higher derivatives of the Green

Table 4. Added mass of ellipses for eccentricities ranging from 0.1 to 1.0 discretized with 16, 32 and 48 segments using the Galerkin method.

n	ϵ	ADDED MASS	EXACT ADDED MASS	ERROR (%)
16	0.10	0.031	0.031	−0.83
32	0.10	0.031	0.031	−0.16
48	0.10	0.031	0.031	−0.07
16	0.20	0.125	0.126	−0.60
32	0.20	0.125	0.126	−0.14
48	0.20	0.126	0.126	−0.07
16	0.30	0.281	0.283	−0.53
32	0.30	0.282	0.283	−0.14
48	0.30	0.283	0.283	−0.07
16	0.40	0.500	0.503	−0.51
32	0.40	0.502	0.503	−0.14
48	0.40	0.502	0.503	−0.07
16	0.50	0.781	0.785	−0.50
32	0.50	0.784	0.785	−0.14
48	0.50	0.785	0.785	−0.07
16	0.60	1.125	1.131	−0.51
32	0.60	1.129	1.131	−0.14
48	0.60	1.130	1.131	−0.07
16	0.70	1.532	1.539	−0.51
32	0.70	1.537	1.539	−0.14
48	0.70	1.538	1.539	−0.07
16	0.80	2.000	2.011	−0.51
32	0.80	2.008	2.011	−0.14
48	0.80	2.009	2.011	−0.07
16	0.90	2.532	2.545	−0.51
32	0.90	2.541	2.545	−0.14
48	0.90	2.543	2.545	−0.07
16	1.00	3.126	3.142	−0.51
32	1.00	3.137	3.142	−0.14
48	1.00	3.140	3.142	−0.07

function is small, they can be used in the single-node integration formula to decrease the quadrature error by including higher-order terms in the Taylor series expansion of the integrand with respect to the x and ξ variables around the centroids of the i-th and jth panels respectively. Recurrence relations with respect to the derivative order exist for the Green functions defined in Section 2. The number of elements in the $N \times N$ Galerkin matrices S and G which correspond to 'distant' panels, grows like N^2 while the number of elements which correspond to 'neighbouring' panels grows like N. Thus for large N, the computational effort in the set-up of the collocation and the Galerkin matrices is comparable. To this we must add the effort required for the solution of the linear system, which is the same for both methods and, unless an iterative solution of the linear system is available, it dominates the total computational effort for large N.

The Galerkin technique may be attractive in applications where the solutions of the source-distribution and the Green problems are both useful. For example, the velocity potential may be desired in order to evaluate the local acoustic pressure field or the local wave load on an offshore structure. In this case the solution of the Green equation is more efficient since the left and right-hand sides of equation (3.5) can be set up simultaneously, circumventing the need to generate and store the matrix S. This is necessary in the source-distribution method, unless the matrices S and D are evaluated separately which may be uneconomical. The velocity field, on the other hand, is desired in the evaluation of the pressure gradient on a lifting surface or of the wave-drift forces on a floating structure. In such cases, the source-distribution method

appears to be more attractive. Knowledge of the source strength permits the differentiation of equation (3.1) to obtain the flow velocities by utilizing single derivatives of the Green function. The evaluation of double derivatives is necessary if the Green equation is used. The Galerkin technique permits the transition from the source-distribution to the Green method by simply transposing the solution matrix and using the proper right-hand side vector.

Acknowledgements

Financial support for this study was provided by the David W. Taylor Ship Research and Development Center (Contract N00167-84-R-0144), the Office of Naval Research (Special Focus in Ship Hydrodynamics, Contract N0014-822-K-0198) and the National Science Foundation (Grant 8210649-A01-MEA). The author expresses his appreciation for this support.

References

1. H. Lamb: *Hydrodynamics*, 6th ed, Dover, New York (1945).
2. J.L. Hess, A.M.O. Smith: Calculation of potential flows around arbitrary bodies, *Prog. Aeronaut. Sci.* 8 (1966) 1–139.
3. L. Morino and C.C. Kuo: Subsonic potential aerodynamics for complex configurations: a general theory, *AIAA J.* 12 (1974) 191–197.
4. J.V. Wehausen and E.V. Laitone: Surface Waves, in: *Encyclopedia of Physics*, Vol. 9, Springer-Verlag (1960).
5. J.N. Newman: Algorithms for the free-surface Green function, *J. Engg. Math.* 19 (1985) 57–67.
6. D. Kolton and R. Kress: *Integral Equations in Scattering Theory*, Wiley-Interscience (1983).
7. A. Barnel, Boundary-integral methods for solving potential flows, Master's Thesis, Massachusetts Institute of Technology, Cambridge Massachusetts (1984).
8. S.R. Breit, J.N. Newman and P.D. Sclavounos: A new-generation panel programs for radiation-diffraction problems in three dimensions, *Proc. Boss'85 Conf. Delft* (1985).